17 Epidermal Reconstruction During Ex Vivo Confocal Microscopy for Detection of Superficial Basal Cell Carcinoma with 3D-Mosaicking and Intensity Projection

Matthew Moronta, Ucalene Harris, Mercedes Sendín-Martín, Alex Bang, Anthony Rossi, Erica Lee, Kishwer Nehal, Chih-Shan Jason Chen, Milind Rajadhyaksha, Kivanc Kose, and Manu Jain

17.1 Epidermal Flattening

Ex vivo confocal microscopy (EVCM) allows rapid evaluation of freshly excised tissue margins with high sensitivity (73–100%) and specificity (89–100%) for residual basal cell carcinoma (BCC) during staged-excision in Mohs surgery [1–8]. A major limitation encountered in these studies has been the inability to flatten peripheral edges of excised tissue, affecting the evaluation of superficial BCCs (sBCC) [9, 10]. As seen in Fig. 17.1, sBCC is found along the basal layer of the epidermis which is why complete margin visualization is necessary for effective detection. A few mechanical devices [11, 12] have been used to physically flatten the tissue specimens, such as magnets, tissue presses, and tissue cassettes, but these have not been sufficient.

We have developed a digital approach to epidermal flattening incorporating real-time software-based reconstruction of overlaid mosaics, each with incomplete peripheral edges, to yield a final merged mosaic [13]. Around 8–10 mosaics, each with partial epidermis, are spaced ~5 um in depth taking approximately 10–20 min in image acquisition. These mosaics are then merged by applying minimum intensity projection in MATLAB to yield a single digitally reconstructed image conferring visualization of the entire epidermal margin.

As seen in Fig. 17.2, the individual frames of a tissue negative for tumor, obtained from Mohs surgical margin, only show partial epidermis, but through digital reconstruction, the final image in Fig. 17.3a shows the full epidermal margin compared to its corresponding H&E-stained tissue section in Fig. 17.3b. As a result of this digital overlay, there is no loss of details of the dermal structures, such as eccrine and pilosebaceous glands even at high magnification (Fig. 17.4c–d). This approach is especially useful for the detection of sBCC (Figs. 17.2, 17.3, 17.5 and 17.6).

M. Moronta · U. Harris · A. Bang · A. Rossi · E. Lee · K. Nehal · C.-S.J. Chen · M. Rajadhyaksha · K. Kose · M. Jain (✉)
Department of Dermatology, Memorial Sloan Kettering Cancer Center (MSKCC), 530 E. 74th Street, New York, NY 10021, USA
e-mail: jainm@mskcc.org

M. Sendín-Martín
Dermatology Department, Hospital Universitario Virgen del Rocío, Sevilla, Spain

M. Jain et al. (eds.), *Cutaneous Atlas of Ex Vivo Confocal Microscopy*,
https://doi.org/10.1007/978-3-030-89316-3_17

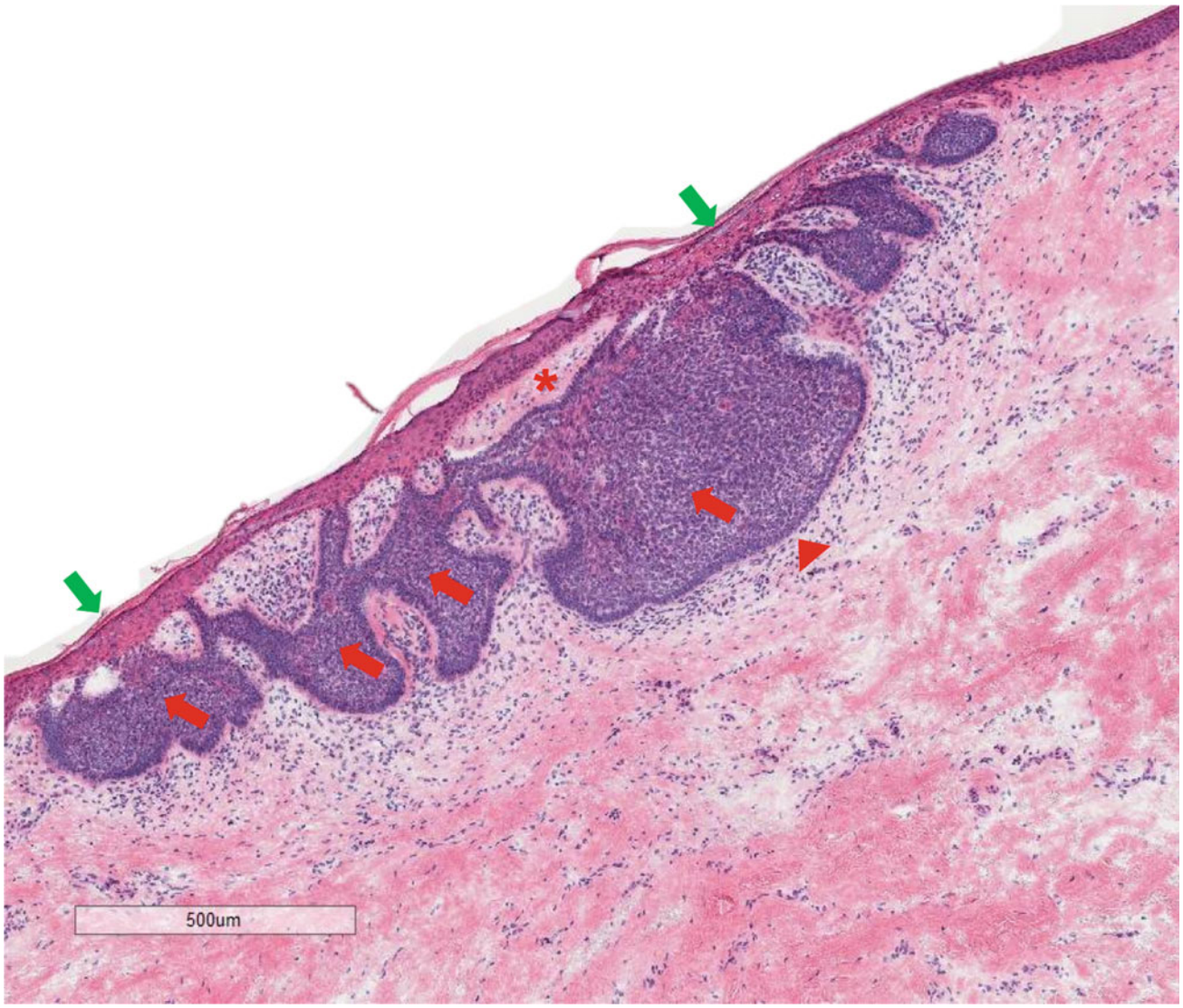

Fig. 17.1 Conventional H&E-stained tissue section of a superficial BCC. H&E image shows a sBCC (red arrow) with clefting (red asterisk) and palisading (red arrowhead) hanging off the epidermal margin (green arrow). Magnification = 10x

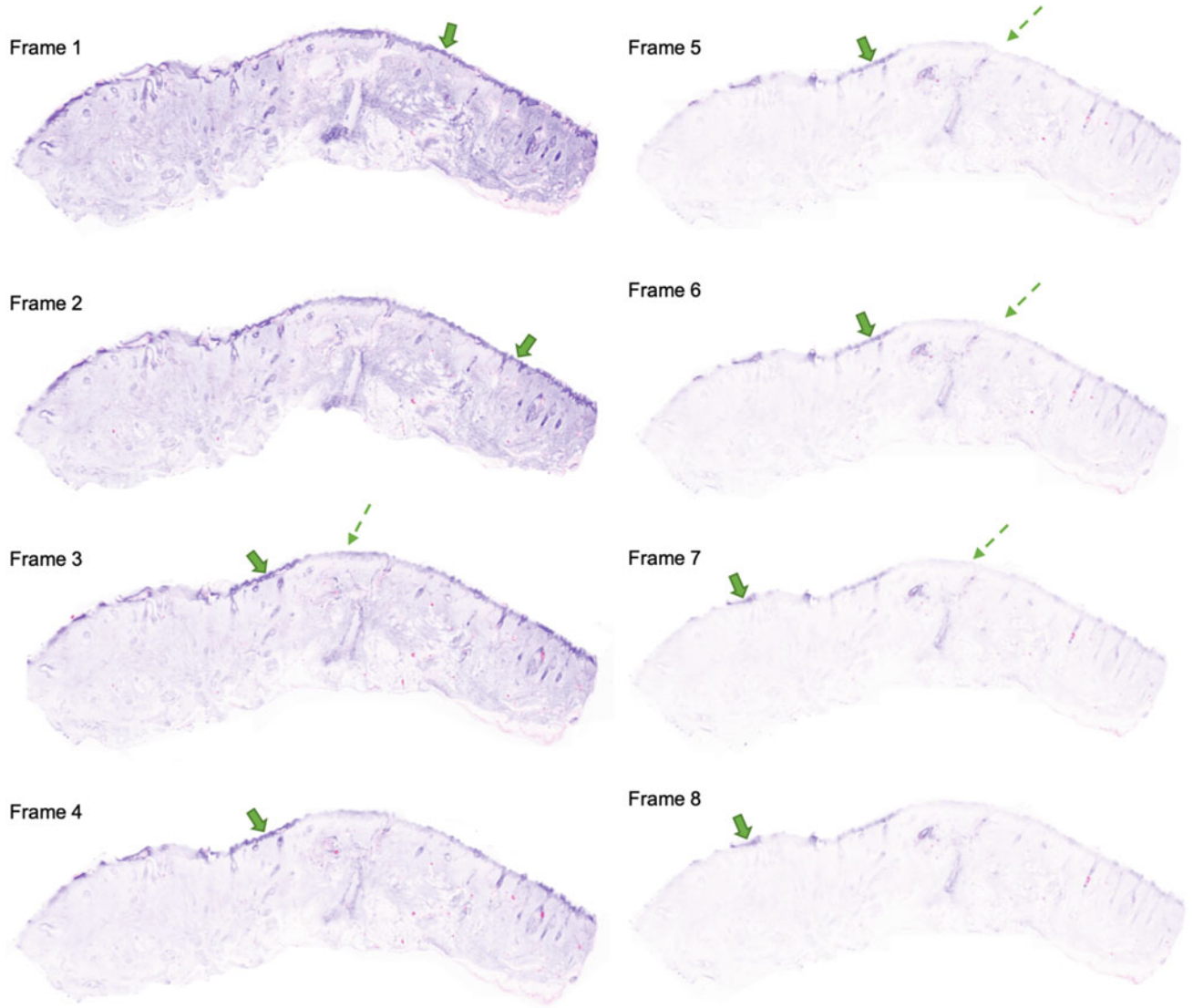

Fig. 17.2 Series of 10 individual digital H&E (DHE) mosaics at varying depths showing partial epidermis from a Mohs negative surgical margin. Digital H&E (DHE) individual mosaics (1.3 × 1.5 mm) spaced at 5 µm in depth show only partial epidermal margin (dashed green arrow) in each frame with areas of full epidermis (solid green arrow)

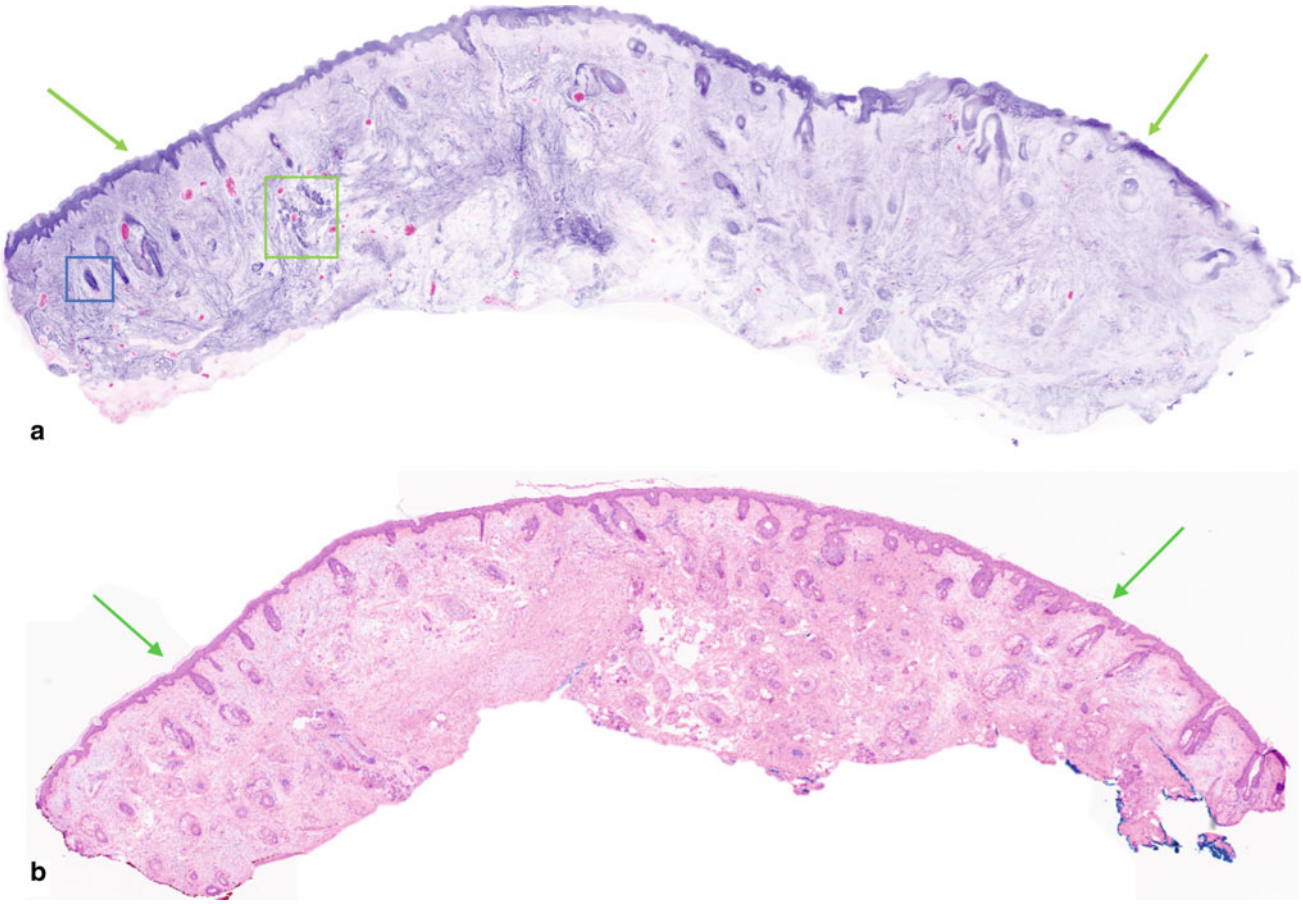

Fig. 17.3 Digitally reconstructed digital H&E (DHE) image of the above 10 individual mosaics (Fig. 17.3) compared to its corresponding H&E image. **a** A reconstructed DHE image was obtained by merging a series of mosaics (1.3 × 1.5 mm) through applying minimum intensity projection to show full epidermal margins (green arrow). Dermal structures such as hair follicle (blue square) and eccrine unit (fluorescent green square) are clearly visible even at this low magnification. **b** Corresponding H&E-stained tissue section (magnification 2x) shows a good correlation with the DHE image for the epidermis (green arrow), hair follicle (black square), and eccrine unit (blue square)

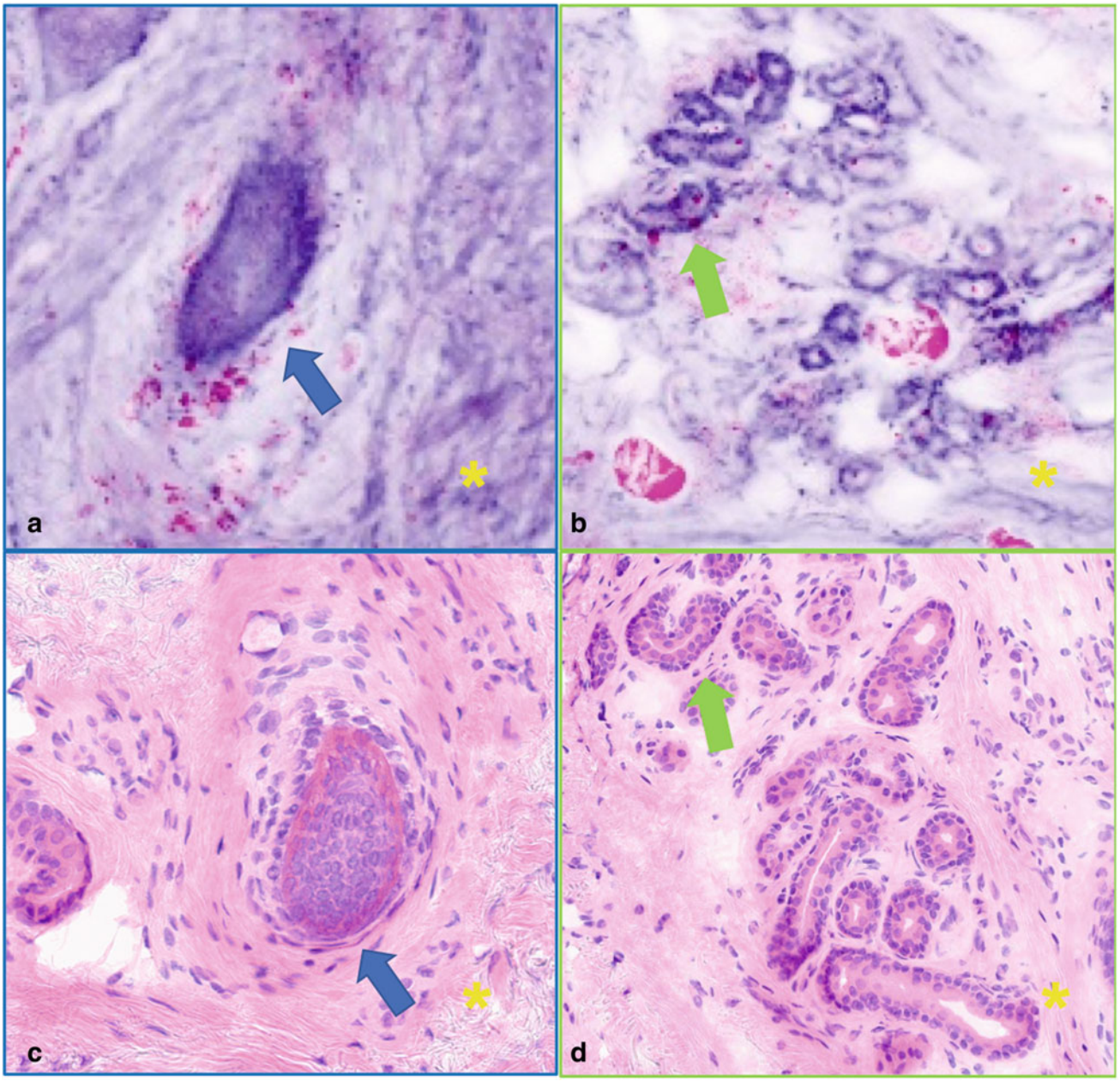

Fig. 17.4 Digitally reconstructed digital H&E (DHE) images of the dermal structures at higher magnification from Fig. 17.3 compared to its corresponding H&E image. **a**, **b** DHE high magnification images of a hair follicle (blue arrow) and an eccrine unit (fluorescent green arrow) within the dermal (yellow asterisk) shows cellular details. **c**, **d** Corresponding H&E images of a hair follicle (blue arrow) and an eccrine unit (fluorescent green arrow) within the dermal (yellow asterisk)

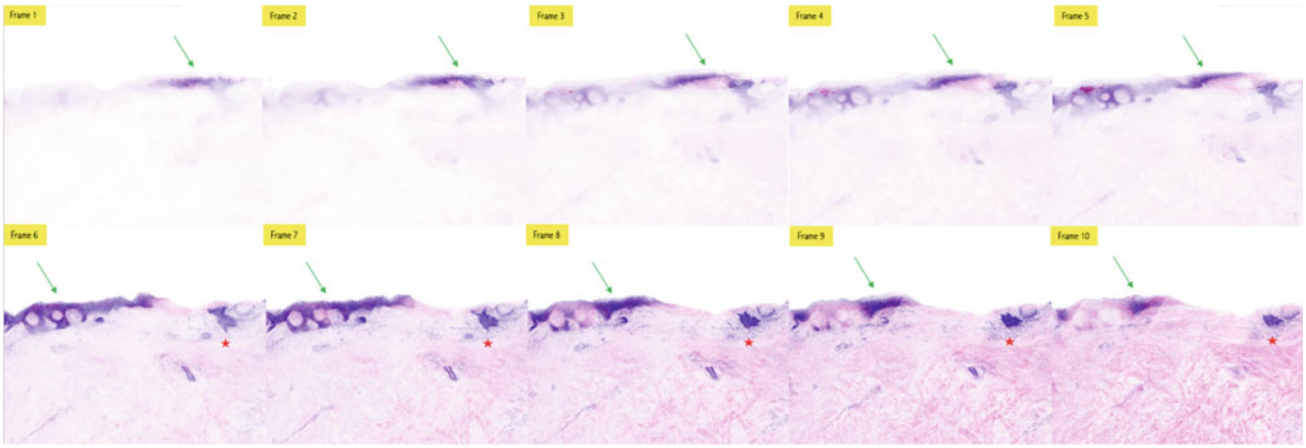

Fig. 17.5 Series of 10 individual sub-mosaics at varying depths showing partial epidermis of a superficial BCC. Digital H&E (DHE) individual mosaics (1.3 × 1.5 mm) spaced at 5 μm in depth show only partial epidermal details (green arrows) in each frame. Notice the presence of sBCC (red star) which is not fully visualized in individual frames. (Reprinted from Sendín-Martín et al. [13]; with permission from Elsevier.)

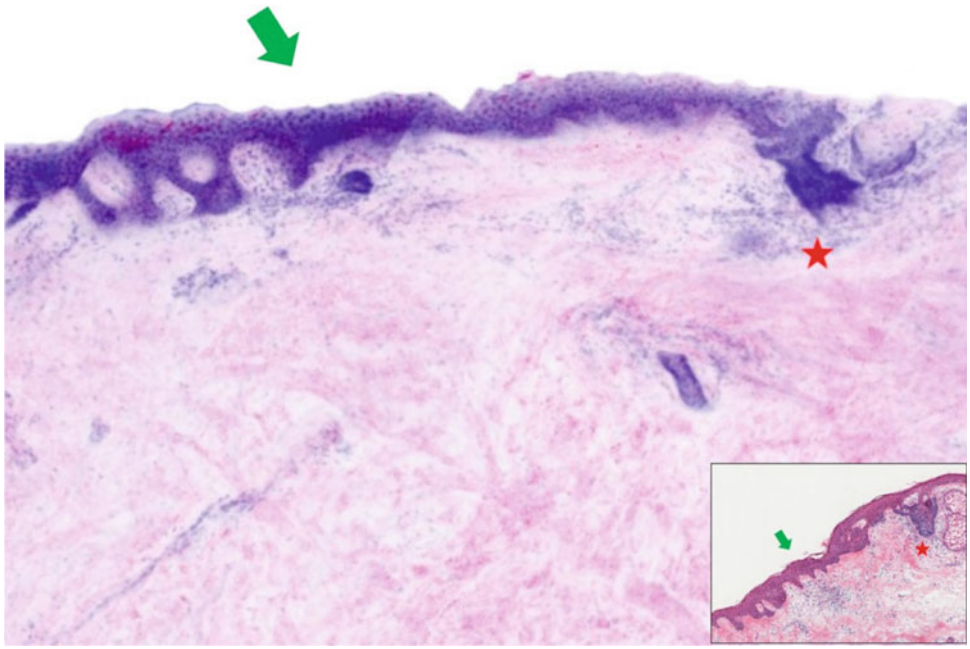

Fig. 17.6 Digitally reconstructed image of a superficial BCC. DHE image reconstructed by merging the series of individual mosaics (1.3 × .1.5 mm) from Fig. 17.5 by applying minimum intensity projection shows the entire epidermis (green arrow) with full visualization of sBCC (red star). The corresponding conventional H&E image can be viewed in the bottom right-hand corner for comparison. (Reprinted from Sendín-Martín et al. [13]; with permission from Elsevier.)

References

1. Karen, et al. Detection of basal cell carcinomas in Mohs excisions with fluorescence confocal mosaicking microscopy. Br J Dermatol. 2009;160(6):1242–50.
2. Larson et al. Detection of skin cancer margins in Mohs excisions with high-speed strip mosaicking confocal microscopy: a feasibility study. Br J Dermatol. 2013;169(4)
3. Bennàssar, et al. Ex vivo fluorescence confocal microscopy for fast evaluation of tumour margins during Mohs surgery. Br J Dermatol. 2014;170(2):360–5.
4. Espinasse, et al. 'En face' ex vivo reflectance confocal microscopy to help the surgery of basal cell carcinoma of the eyelid. Clin Exp Opthalmol. 2017;45:442–7.
5. Longo, et al. Diagnostic accuracy of ex vivo fluorescence confocal microscopy in Mohs surgey of basal cell carcinomas: a prospective study on 753 margins. Br J Dermatol. 2019;180:1473–80.
6. Mu, et al. Use of digitally stained multimodal confocal mosaic images to screen for nonmelanoma skin cancer. JAMA Dermatol. 2016;152(12):1335–41.
7. Peters, et al. Diagnostic accuracy of a new ex vivo confocal laser scanning microscope compared to H&E-stained paraffin slides for micrographic surgery of basal cell carcinoma. JEADV. 2019;33:298–304.
8. Jain M, Rajadhyaksha M, Nehal K. Implementation of fluorescence confocal mosaicking microscopy by "early adopter" Mohs surgeons and dermatologists: recent progress. J Biomed Opt. 2017;22(2):24002. https://doi.org/10.1117/1.JBO.22.2.024002. PMID:28199474;PMCID:PMC5310648.

9. Asgari MM, Moffet HH, Ray GT, Quesenberry CP. Trends in basal cell carcinoma incidence and identification of high-risk subgroups, 1998–2012. JAMA Dermatol. 2015;151:976–81. https://doi.org/10.1001/jamadermatol.2015.1188.
10. Malvehy, et al. Ex vivo confocal microscopy: revolution in fast pathology in dermatology. Br J Dermatol. 2020;2020. https://doi.org/10.1111/bjd.19017.
11. Pérez-Anker J, Puig S, Malvehy J. A fast and effective option for tissue flattening: optimizing time and efficacy in ex vivo confocal microscopy. J Am Acad Dermatol. 2019; 80(27):pii: S0190–9622 (19)31040–0 https://doi.org/10.1016/j.jaad.2019.06.041.
12. Cinotti E, Grivet D, Labeille B, et al. The "tissue press": a new device to flatten fresh tissue during ex vivo confocal microscopy examination. Skin Res Technol. 2017;23(1):121–4. https://doi.org/10.1111/srt.12293.
13. Sendín M, Kose K, Harris U, Rossi A, Lee E, Nehal K, Rajadhyaksha M, Jain M. Complete visualization of epidermal margin during ex vivo confocal microscopy of excised tissue with 3D-mosaicking and intensity projection. J Am Acad Dermatol. 2020. https://doi.org/10.1016/j.jaad.2020.05.044.